

## Cloning, DNA Sequence Determination, and Analysis of Growth-Associated Expression of the *sodF* Gene Coding for Fe- and Zn-Containing Superoxide Dismutase of *Streptomyces griseus*

KIM, JU-SIM AND JEONG KUG LEE\*

Department of Life Science, Sogang University, Seoul 121-742, Korea

Received: August 2, 2000

Accepted: September 15, 2000

**Abstract** Iron- and zinc-containing superoxide dismutase (FeZnSOD) and nickel-containing superoxide dismutase (NiSOD) are cytoplasmic enzymes in *Streptomyces griseus*. The *sodF* gene coding for FeZnSOD was cloned from genomic Southern hybridization analysis with a 0.5-kb DNA probe, which was PCR-amplified with facing primers corresponding to the N-terminal amino acids of the purified FeZnSOD of *S. griseus* and a C-terminal region which is conserved among bacterial FeSODs and MnSODs. The *sodF* open reading frame (ORF) was comprised of 213 amino acids (22,430 Da), and the deduced sequence of the protein was highly homologous (86% identity) to that of FeZnSOD of *Streptomyces coelicolor*. The FeZnSOD expression of exponentially growing *S. griseus* cell was approximately doubled as the cell growth reached the early stationary phase. The growth-associated expression of FeZnSOD was mainly controlled at the transcriptional level, and the regulation was exerted through the 110 bp regulatory DNA upstream from the ATG initiation codon of the *sodF* gene.

**Key words:** Superoxide dismutase, FeZnSOD, *Streptomyces griseus*, *sodF*, growth-associated expression, transcriptional regulation

Cellular metabolism of molecular oxygen may result in the generation of reactive oxygen species, such as superoxide anion ( $O_2^-$ ), hydroxyl radical (OH), and hydrogen peroxide ( $H_2O_2$ ), because of the incomplete reduction of oxygen during respiration. The cellular damage resulting from these reactive oxidants includes DNA strand breakage, protein inactivation, and the peroxidation of membrane lipids, to mention just a few [4, 32]. One defense system developed by most organisms is to remove the reactive oxidants using enzymes such as superoxide dismutase (SOD),

catalase, and peroxidase. SOD converts  $O_2^-$  into  $H_2O_2$  and  $O_2$  [32], catalase degrades  $H_2O_2$  to  $H_2O$  and  $O_2$ , and peroxidase decomposes  $H_2O_2$  utilizing various electron donors [11].

Three types of SODs have been identified according to their active metals. Bacteria have manganese-containing SOD (MnSOD) and iron-containing SOD (FeSOD) in their cytoplasm, whereas copper- and zinc-containing SOD (CuZnSOD) is located in the periplasm of several bacteria including *Escherichia coli* [14], *Caulobacter crescentus*, and some pseudomonads [30, 31]. It is believed that CuZnSOD works in the periplasm to remove exogenous superoxide, while MnSOD and FeSOD prevent intracellular DNA, proteins, and membrane lipids from oxidation [28]. CuZnSOD is characteristic of the cytosols of eukaryotic cells and mitochondrial intermembrane space, while MnSOD is located in the mitochondrial matrix. In addition, higher plants contain CuZnSOD in chloroplast [4]. MnSOD and FeSOD are very closely related in their amino acid sequences, yet quite distinct from CuZnSOD [24]. The expression of SODs has been analyzed in many organisms. In *E. coli*, the expression of MnSOD (*sodA*) displays oxygen responsiveness. Its FeSOD (*sodB*) is constitutively expressed under most growth regimes, while CuZnSOD (*sodC*) increases noticeably during the stationary phase due to elevated transcription [14].

In *Streptomyces* spp., highly aerobic soil bacteria, two novel SODs were found; nickel-containing (NiSOD) and iron- and zinc-containing (FeZnSOD) enzymes. NiSOD and FeZnSOD, in both *Streptomyces griseus* [35] and *Streptomyces coelicolor* [17], were identified as homotetramers of about 13- and 22-kDa subunits, respectively. In *S. coelicolor* Müller, the transcription of the gene coding for NiSOD (*sodN*) was increased by nickel, which also plays an important role in processing the enzyme in addition to acting as a catalytic cofactor [18]. FeZnSOD expression of *S. coelicolor* Müller was regulated through the repression of the coding gene (*sodF*) transcription by nickel [19].

\*Corresponding author  
Phone: 82-2-705-8459; Fax: 82-2-704-3601;  
E-mail: jgklec@ccs.sogang.ac.kr

In the present study, *sodF* of *S. griseus* was cloned and sequenced, and the gene expression was analyzed to understand more clearly the regulatory expression and role of FeZnSOD in relation to the growth phase. Results showed that the FeZnSOD expression increased approximately twofold during the growth transition from the exponential to the early stationary phase. The growth-associated expression appeared to be controlled at the level of *sodF* transcription, and the growth-responsive *cis* DNA was localized within a 110 bp DNA upstream from the ATG initiation codon of the gene.

## MATERIALS AND METHODS

### Bacterial Strains and Growth Conditions

*S. griseus* KCTC 9006 was obtained from the Korean Collection for Type Cultures (KCTC). The *sodF*-disrupted cell of *S. lividans* TK24 [19] was provided by Dr. J.-H. Roe (Seoul National University, Korea). The cells were grown basically and aerobically at 28°C for *S. griseus* [35] and at 37°C for the *sodF*-disrupted cell of *S. lividans* in the presence of apramycin (25 µg/ml), as previously described [19]. For broth culture, YEME medium (pH 7.0) containing 0.5% yeast extract, 0.5% casamino acid, 0.5% Bacto-peptone, 0.3% malt extract, 2.5 mM MgCl<sub>2</sub>, and 1% glucose was inoculated with a spore suspension (about 10<sup>5</sup> spores/ml) collected from a YEME plate grown for 5 days. The cell growth was monitored through the optical density of culture at 600 nm. *S. lividans* was transformed with plasmids as described previously [12]. Thiostrepton (Ts) was used at 50 µg/ml to select and maintain the *S. lividans* cell carrying the plasmid-encoding Ts' gene.

*E. coli* was grown at 37°C in Luria-Bertani medium [27]. Streptomycin (Sm), spectinomycin (Sp), and ampicillin (Ap) were added to the culture at each final concentrations of 50 µg/ml, for the drug resistance genes.

### DNA Manipulation and Sequence Analysis

*S. griseus* genomic DNA was prepared as described previously [12]. The polymerase chain reaction (PCR) mixture contained 500 ng of the *S. griseus* genomic DNA, 500 pmol of each of the facing primers, 2.5 mM of deoxynucleotide triphosphates, and 5 U of *Taq* DNA polymerase (Takara, Japan) per 50 µl of the reaction buffer supplied by Takara. To facilitate the denaturation of G+C-rich DNA, dimethylsulfoxide (DMSO) was added to the reaction mixture at a final concentration of 10% [9]. The PCR was performed with 30 cycles of the following three-step cycle: 1 min at 94°C, 1 min at 60°C, and 2 min at 68°C.

*S. griseus* genomic DNA was digested to completion with appropriate restriction enzymes and electrophoresed on 0.8% agarose gels. Southern blot on to a Hybond-N membrane (Amersham Pharmacia Biotech, Piscataway, NJ, U.S.A.) was performed as previously described [27]. A DNA labeling

and detection kit was obtained from Amersham Pharmacia Biotech and used according to the manufacturer's instructions.

DNA sequence was determined with an ALFexpress automatic DNA sequencer (Amersham Pharmacia Biotech). The dideoxynucleotide sequencing reaction was carried out with double-stranded DNA using the T7 DNA polymerase of a Cy5™ AutoRead™ sequencing kit (Amersham Pharmacia Biotech). The determined nucleotide sequence was assembled and analyzed using the DNASIS program (Version 7.0) (Promega, Madison, WI, U.S.A.).

### RNA Isolation, Quantification, and Northern (RNA) Hybridization Analysis

The total RNA from *S. griseus* was extracted as described by Horinouchi *et al.* [13]. For determining mRNA half-life, rifampicin was added to the culture at a final concentration of 200 µg/ml. Portions (25 ml) were removed at 10 min intervals for 40 min, and the total RNA was prepared. The RNA concentration was measured by orcinol assay.

Ten micrograms of the denatured RNA sample per lane was electrophoretically separated on 1% (w/v) agarose-2.2 M formaldehyde gels, and transferred to a nylon membrane (Schleicher and Schuell, Dassel, Germany). A strand-specific RNA probe using [ $\alpha$ -<sup>32</sup>P]CTP (Amersham Pharmacia Biotech, Piscataway, U.S.A.) was prepared according to the manufacturer's instructions with an RNA transcription kit (Stratagene, La Jolla, CA, U.S.A.) and pBS (Stratagene) clones. The prehybridization, hybridization, and washing procedures were also performed according to the protocols suggested by the manufacturer (Stratagene). Quantification of signals was performed using the Tina 2.0 program of a BIO-Imaging Analyzer (FUJI, Japan). The *sodF*-specific signals were normalized to those generated with a probe specific for 16S rRNA, of which DNA was derived from *S. griseus* KCTC 9080 [16].

### Detection of Catechol Dioxygenase Activity

The regulatory DNA of *sodF* was transcriptionally fused to a promoterless copy of the *xylE* gene on a low-copy number plasmid pXE4 [15]. The pXE4-derived plasmid was then mobilized into *S. lividans* as previously described [12]. The transformed cells grown on the YEME broth were broken by sonication, and catechol dioxygenase activities were measured as previously described [15]. All the experiments involving catechol dioxygenase assays were carried out in duplicate in at least two separate experiments.

### Detection of SOD Activity, Purification of SOD, Preparation of Antiserum, and Western Immunoblot Analysis

The activity staining of SOD in a native polyacrylamide gel (10% [w/v] acrylamide) was performed according to the method of Beauchamp and Fridovich [3]. FeZnSOD of *S. griseus* was purified and used as an immunogen to

obtain an antiserum as previously described [35]. Preparation of the cell-extracts, electrophoresis (SDS-PAGE), and electrotransfer of proteins were also performed according to the methods as described previously [7, 23, 27, 35]. A blot treated with the FeZnSOD-specific antibody was reacted with a 1/2,000 dilution of goat anti-mouse IgG (Pierce, Fockford, IL, U.S.A.) conjugated with horseradish peroxidase. Then, the FeZnSOD polypeptide was identified with an ECL detection system supplied by Amersham Pharmacia Biotech. Protein was determined by a modified Lowry method using bovine serum albumin as the standard [21]. The relative activities and protein levels of FeZnSOD between samples were quantified by scanning the gel and blot with the Tina 2.0 program of a BIO-Imaging Analyzer (FUJI).

## RESULTS

### *sodF* Gene Cloning

A 0.5-kb DNA corresponding to a portion of the *sodF* gene of *S. griseus* was obtained using PCR with two facing primers; SOD1, 5'-GCNACNTA[T/C]ACNCTNCC-3', and SOD2, 5'-TA[A/G]TANGC[A/G]TG[T/C]TCCCA-3'. The SOD1 was designed from N-terminal six amino acids of the purified FeZnSOD of *S. griseus* [35], while the SOD2 reflected the amino acid sequence, WEHAYY, of a conserved region among bacterial FeSODs and MnSODs [24] (Fig. 1). Using the 0.5-kb DNA as a probe, a 1.1-kb *SalI-SmaI* DNA fragment (Fig. 2A) was obtained through colony hybridization from genomic DNA libraries in which *S. griseus* DNA had been digested with the restriction enzymes and cloned into pBS (Stratagene).

The 1.1-kb *SalI-SmaI* DNA was cloned into pWHM3, a shuttle plasmid between *E. coli* and *Streptomyces* spp. [34], to generate pWHM365. The FeZnSOD expression was examined with the pWHM365 *in trans* in a *sodF*-disrupted cell of *S. lividans* TK24. As shown in Fig. 2B, the *sodF*-disrupted cell containing pWHM365 exhibited FeZnSOD activity (lane 1), which comigrated with that of *S. griseus* in a nondenaturing polyacrylamide gel (lane 3). Thus, the entire *sodF* gene of *S. griseus* was localized to the 1.1-kb DNA. The FeZnSOD polypeptide expressed from pWHM365 was detected in immunoblot hybridization analyses with an antiserum against *S. griseus* FeZnSOD (Fig. 2C, lane 1). As expected, neither activity nor protein specific to FeZnSOD was observed with pWHM3 as a control (Fig. 2B and 2C, lanes 2). The level of the FeZnSOD protein observed with pWHM365 was approximately seven times higher than that of the *S. griseus* cells (Fig. 2C, lanes 1 and 3). Likewise, four times more activity of FeZnSOD was detected with the cloned gene (Fig. 2B, lanes 1 and 3). The higher expression of FeZnSOD by the cloned gene was attributed to the copy number of the plasmid. The

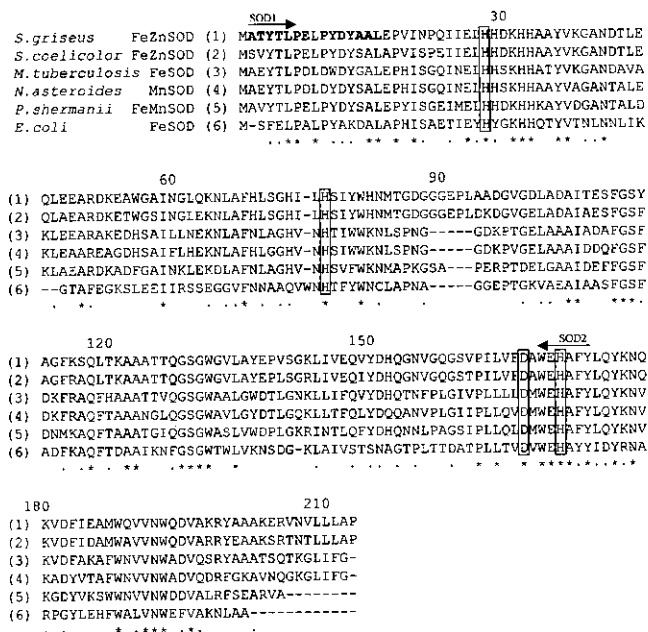


Fig. 1. Deduced amino acid sequence of *S. griseus* FeZnSOD and comparison with those of other bacterial SODs.

The sequence alignment was obtained using the CLUSTAL W (version 1.70) program. The residues conserved in all six sequences are indicated with asterisks, while similar amino acids are marked with dots. The four amino acids of the metal ligands are indicated in boxes. The residues corresponding to the N-terminal amino acid sequence determined by Edman degradation with the purified *S. griseus* FeZnSOD [35] are shown in boldface letters. The facing arrows above the amino acid sequence indicate the two primers, SOD1 and SOD2, which were included in the PCR amplification to get a 0.5-kb DNA fragment internal to the *sodF* gene. The amplified 0.5-kb DNA was used as a probe to clone the whole *sodF* gene (see text).

NiSOD activity of *S. griseus* was observed at a location different from that of *S. lividans* (Fig. 2B).

### Homology Comparisons with other SOD Proteins

From the sequence analysis of the 1.1-kb *SalI-SmaI* DNA, the ORF of the *sodF* gene was located as shown in Fig. 2A. The nucleotide sequence of the DNA fragment was assigned as GenBank accession no. AF141866. The ORF started 420 nucleotides downstream from the *SalI* site and encoded a polypeptide of 213 amino acids (Fig. 1). The N-terminal amino acid sequence deduced from the nucleotide sequence was consistent with that determined for purified FeZnSOD [35] except for the first residue of methionine and the ninth residue of leucine. The methionine may be removed for maturation, as has been observed for other bacterial SODs [5, 33]. The predicted polypeptide of 212 amino acids with an alanine as a N-terminus showed a calculated molecular mass of 23,343 Da, which is close to that of purified FeZnSOD, as estimated by SDS-PAGE (22.0 kDa) [35].

Homology comparison with other SOD proteins revealed that the FeZnSOD of *S. griseus* is similar to SODs from various bacteria. Five representative sequences are shown in Fig. 1. The deduced amino acid sequence of the FeZnSOD

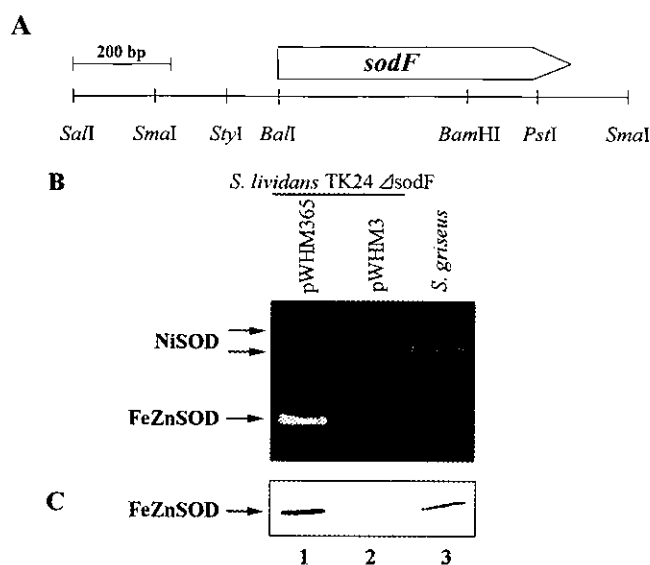


**Fig. 2.** Localization of *sodF* within 1.1-kb *SalI*-*SmaI* DNA of *S. griseus*.

(A) Restriction map of the *sodF* DNA. (B) FeZnSOD activity detected with the cloned gene *in trans* in *sodF*-disrupted cell of *S. lividans* TK24 and compared with that of *S. griseus*. All the strains were grown in YEME broth until the early stationary phase. The SOD activities were detected in a nondenaturing polyacrylamide (10%) gel loaded with cell extracts (20  $\mu$ g protein per lane) from *S. griseus* (lane 3), the *S. lividans* *sodF*-disrupted cell containing pWHM365 (lane 1), and pWHM3 (lane 2). (C) Immunoblot analysis of the same extracts (7  $\mu$ g protein per lane) as in (B) with mouse antiserum against the purified FeZnSOD polypeptide of *S. griseus*.

of *S. griseus* showed the highest homology to that of FeZnSOD of *S. coelicolor* Müller [19] with an 86% identity and 93% similarity. It exhibited about 69% similarity to the FeSOD from *Mycobacterium tuberculosis* [36] and a 66% similarity to the SODs from *Nocardia asteroides* and *Propionibacterium shermanii* [1, 22]. The SOD from *N. asteroides* is reported to contain an equimolar amount of Fe, Mn, and Zn [2], while *P. shermanii* produces a cambialistic SOD, the metal cofactor of which can be substituted according to the metal supply of the culture medium as previously reported [22]. *E. coli* FeSOD [6] showed 49% similarity. These six sequences shared 48 identical residues. The invariant amino acids also comprise four amino acids, which are known to be metal ligands (three histidine residues and one aspartic acid residue) [29] and are conserved at the positions indicated by the boxes in Fig. 1.

#### Expression of FeZnSOD during Growth of *S. griseus*

The activity and level of protein specific to the *S. griseus* FeZnSOD were examined using the extracts from cells during the exponential and early stationary phase of growth. The cells in the early stationary phase showed about two times more activity and protein than the exponentially growing cells (Fig. 3A and 3B). Thus, the change of FeZnSOD activity during cell growth was due to the increase of the protein level. The NiSOD activity also

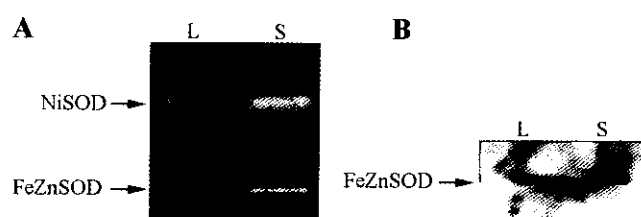


**Fig. 3.** FeZnSOD expressions associated with growth phase.

(A) The SOD activities were detected using cell extracts (20  $\mu$ g protein per lane) from *S. griseus* cells harvested during the mid-logarithmic (L,  $A_{600}$  between 0.5 and 1.0) and early stationary (S,  $A_{600}$  between 1.5 and 1.9) phase of growth in YEME broth. (B) Immunoblot analysis of proteins (7  $\mu$ g protein per lane) in the same extracts as in (A) with the antiserum against the FeZnSOD of *S. griseus*.

increased about twofold following the same growth transition (Fig. 3A). The increased activities of both FeZnSOD and NiSOD might reflect physiological response to protect cells against the superoxide radicals that are accumulated during the stationary phase of growth [8, 10].

#### Regulation of *sodF* Transcription during Growth

Northern (RNA) hybridization analysis was performed with a strand-specific RNA probe (Fig. 4A, probes *a*) to identify the transcriptional activity of the *sodF* gene. The probe spanned most of the *sodF* structural gene as well as its 254 bp upstream DNA. Total RNA was isolated from *S. griseus* cells during the exponential and early stationary phases of growth. A transcript of approximately 0.8 kb (Fig. 4B) was observed. The determination of the blot signals revealed that the cells in the early stationary phase contained about two times more transcript than the cells during exponential growth.

#### Stability of *sodF* Transcript

The *sodF* transcript level varied in relation to the growth phase. Since this change could be exerted by either the synthesis or stability of the transcript, the decay rates of the transcript were determined to distinguish between these two possibilities. To block further RNA synthesis, rifampicin was added to the *S. griseus* cells during the exponential or early stationary phase of growth. Total RNAs were extracted from the cells harvested at 10-min intervals for 40 min after the addition of rifampicin. The amount of RNA transferred and its detection with a *sodF*-specific RNA probe (Fig. 4A, probe *a*) were within a linear assay range. The half-lives of the transcript were estimated to be between 6 to 7 min, irrespective of the growth phase (Fig. 5). Consequently, the elevated FeZnSOD expression during the early stationary phase would appear to be mainly regulated by *sodF* transcription rather than by the stability of transcript.

#### Analysis of *cis* DNA Responsible for Growth-Associated Regulation of *sodF* Transcription

To locate a *cis* DNA responsible for growth-associated transcriptional regulation, the *sodF* upstream DNA of *S.*

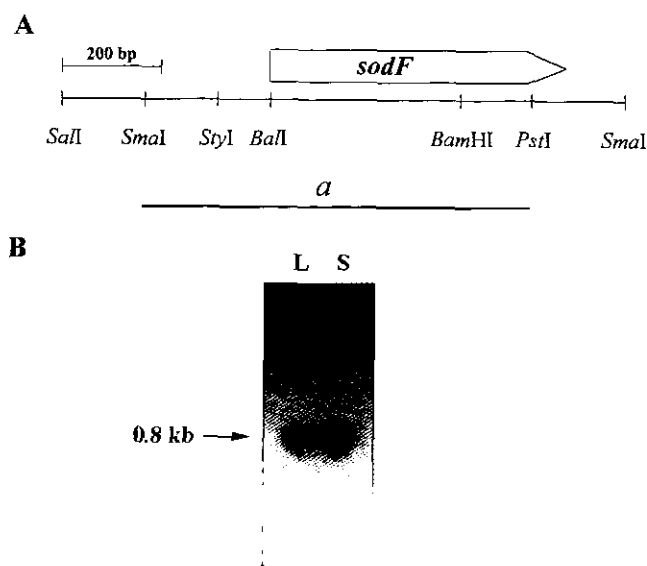


**Fig. 4.** Identification of *sodF* transcript and its level change in relation to the growth phase.

(A) Location of an RNA probe *a*. (B) Northern blot hybridization analysis with [ $\alpha$ - $^{32}$ P]CTP-labeled RNA probe. Total RNA was prepared from *S. griseus* cells during the logarithmic (L) and early stationary (S) phases of growth. The culture absorbencies of the growth phases, when the cells were harvested, were mentioned in Fig. 3.

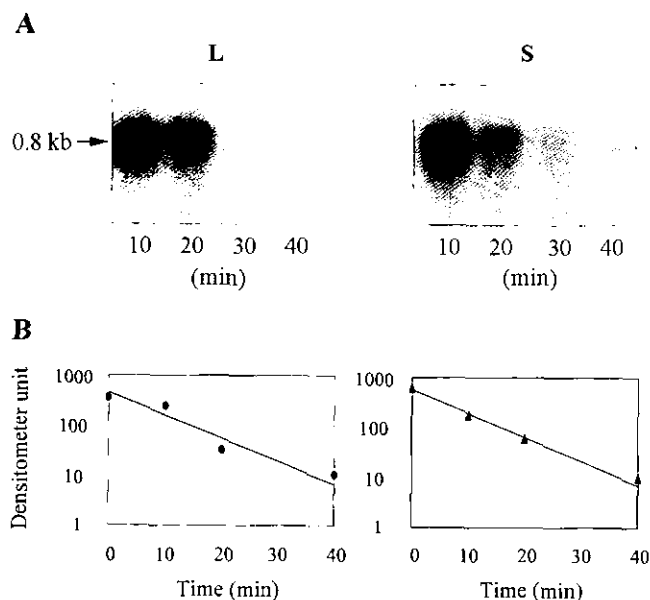


**Fig. 5.** Stability determination of *sodF* transcript.

*S. griseus* cells were cultured in YEME broth. Rifampicin, an inhibitor of RNA synthesis, was added to each culture during the logarithmic (L) and early stationary (S) phases of growth. The culture absorbencies of each phase, when the cells were sampled, were the same as in Fig. 4. (A) The cells were harvested at 10-min intervals for 40 min after the addition of rifampicin and the total RNA was extracted. Northern blot hybridization was performed with the *sodF*-specific RNA probe *a* (Fig. 4A). Note that each lane of blot L was loaded with 15  $\mu$ g of RNA, while blot S contained 10  $\mu$ g of RNA per lane. (B) The transcript levels of the cells during the logarithmic (●) and early stationary (▲) phases are shown by semi-logarithmic plots.

*griseus* was limited by two restriction sites, *SaII* and *StyI*, and transcriptionally fused to a promoterless copy of the *xylE* gene on a low-copy number plasmid pXE4 [15]. pJJK365 contained the *sodF* regulatory DNA from -421 (*SaII*) to +4 (*BaII*) relative to the ATG initiation codon and pJJK054 contained the DNA from -110 (*StyI*) to the same 3' site, *BaII* (Fig. 6A). Since the growth-associated expression of FeZnSOD was similarly regulated in both *S. griseus* and *S. lividans* (data not shown), each plasmid was mobilized into *S. lividans*, a generally recognized expression host, and then examined for catechol dioxygenase activities with respect to the upstream DNAs. During the exponential and early stationary phases of growth, the cells were broken by sonication and catechol dioxygenase activities were measured. No enzyme activity was detected when the *xylE* of pXE4 was cloned immediately downstream from the transcription-translation stop DNA,  $\Omega$  Sm'/Sp' [25] (data

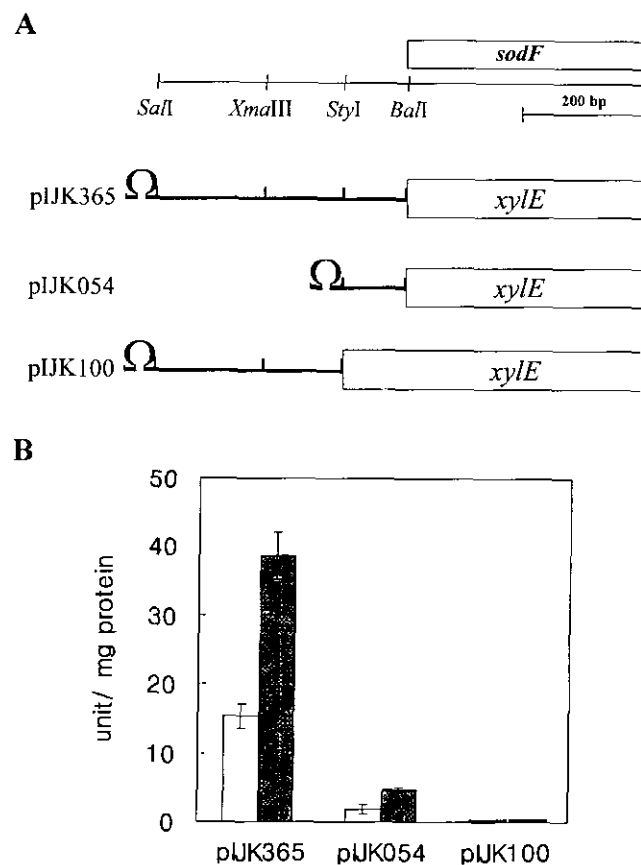


**Fig. 6.** Analysis of *sodF*::*xylE* fusions to localize *cis* DNA for growth-responsive transcriptional regulation.

(A) *sodF* DNA fragments transcriptionally fused to *xylE*. A transcription-translation stop DNA,  $\Omega$  Sm'/Sp', was cloned at the border between the vector and the *sodF* upstream DNA to block any fortuitous transcriptional readthrough from the vector DNA. (B) Histogram showing the catechol dioxygenase activities of each plasmid in *S. lividans* cells harvested during the logarithmic (open bar;  $A_{600}$  between 0.5 and 1.0) and early stationary (solid bar;  $A_{600}$  between 1.5 and 1.9) phases of growth in YEME broth. Standard deviations of the activities are shown on each bar.

not shown). The catechol dioxygenase activities of the two plasmids, pJJK365 and pJJK054, were increased approximately twofold during the growth transition from the exponential to early stationary phase (Fig. 6B). These results imply that the regulatory DNA downstream from the *StyI* (-110) of pJJK054 appears to contain a promoter as well as a *cis* DNA involved in growth-responsive transcriptional regulation. It remains to be determined whether they are the same DNA region or not. The possibility of the presence of another promoter at the DNA upstream from the *StyI* site has been excluded, since no enzyme activity was observed with pJJK100 (Fig. 6B), in which the 311 bp *SalI-StyI* DNA was fused to the *xylE* (Fig. 6A). In addition, the primer extension analysis of the *sodF* transcript localized its 5' end at the DNA downstream from the *StyI* (-110) site, based on the size estimation of an extended product (data not shown). It should be noted that the inclusion of the upstream DNA from -110 (pJJK054) to -421 (pJJK365) resulted in a near sevenfold higher-level expression of catechol dioxygenase activities. Thus, it would appear that 311 bp *SalI-StyI* DNA contained a putative activator-binding sequence(s) because of the higher level of *sodF* transcription.

## DISCUSSION

Two novel SODs, NiSOD and FeZnSOD, from *S. griseus* have been previously purified and characterized [35]. In this work, the *sodF* gene coding for FeZnSOD of *S. griseus* was cloned and sequenced in order to elucidate the regulatory mechanism of FeZnSOD expression. It was concluded that the FeZnSOD expression during growth was mainly controlled at the level of the synthesis of *sodF* mRNA, since variations in the activity and levels of protein specific to FeZnSOD were reflected by changes in the transcript level. In addition, the stability of the *sodF* transcript was not altered significantly under the experimental conditions examined (Fig. 5).

Both the FeZnSOD and NiSOD activities of *S. griseus* increased approximately twofold following growth from the exponential to early stationary phase. The increased activities of these SODs may reflect a physiological response to protect the cells from higher accumulation of superoxide radicals, which can occur during the stationary phase of growth [8, 10]. Both activities were further examined during succeeding 50 h after the early stationary phase. The FeZnSOD activity decreased twofold in the stationary phase and then maintained a plateau. However, the NiSOD activity maintained an elevated level throughout the stationary phase examined (Kim and Lee, unpublished result). Accordingly, the total SOD activity would seem to be the highest during the early stationary phase. In addition, the NiSOD might be a primary SOD during the stationary phase of aerobiosis.

Highly aerobic soil bacteria, Streptomycetes, have been characterized by the production of a variety of secondary

metabolites, including antibiotics, during the stationary phase of cell growth [26], where morphological and physiological differentiations are usually induced by the limitation of essential nutrients such as carbon, nitrogen, and phosphate (for a review, see [20]). An association between the SOD expression and the process of differentiation has not yet been revealed.

As shown in Fig. 6, the 311 bp DNA between the *SalI* and *StyI* sites appeared to be required for the activation of *sodF* transcription irrespective of the growth phase. This DNA was further analyzed and it was found that the same 311 bp DNA was responsible for the increased expression of FeZnSOD following treatment with plumbagin, a superoxide generator (Kim and Lee, unpublished result). It remains to be determined whether the *cis* area for transcriptional activation is the same site(s) as that responsible for the increased expression by plumbagin.

In summary, the regulation of FeZnSOD expression of *S. griseus* was examined with respect to the growth phase, and it was found that the expression was mostly controlled at the level of *sodF* transcription. In addition, the *cis* DNA for the growth-associated regulation of *sodF* transcription was localized. This *cis*-acting DNA will facilitate the identification of transcriptional regulator(s), which may be a sigma factor(s) or other activator(s) that can recognize the growth phase and induce the *sodF* transcription.

## Acknowledgments

This work was supported by a research grant (1998) given from the Korea Research Foundation to the Research Institute for Basic Sciences at Seoul National University.

## REFERENCES

1. Alcendor, D. J., G. D. Chapman, and B. L. Beaman. 1995. Isolation, sequencing and expression of the superoxide dismutase-encoding gene (*sod*) of *Nocardia asteroides* strain GUH-2. *Gene* **64**: 143-147.
2. Beaman, B. L., S. M. Scates, S. E. Moring, R. Deem, and H. P. Misra. 1983. Purification and properties of a unique superoxide dismutase from *Nocardia asteroides*. *J. Biol. Chem.* **258**: 91-96.
3. Beauchamp, C. and I. Fridovich. 1971. Superoxide dismutase: Improved assays and an assay applicable to acrylamide gels. *Anal. Biochem.* **44**: 276-287.
4. Bertini, I., H. B. Gray, S. J. Lippard, and J. S. Valentine. 1994. *Bioinorganic Chemistry*, pp. 260-311. University Science Books, Mill Valley, CA, U.S.A.
5. Bowler, C., L. V. Kaer, W. V. Camp, M. V. Montagu, D. Inze, and P. Dhaese. 1990. Characterization of the *Bacillus stearothermophilus* manganese superoxide dismutase gene and its ability to complement copper/zinc superoxide dismutase

- deficiency in *Saccharomyces cerevisiae*. *J. Bacteriol.* **172**: 1539–1546.
6. Carlouz, A., M. L. Ludwig, W. C. Stallings, J. A. Fee, H. M. Steinman, and D. Touati. 1988. Iron superoxide dismutase: Nucleotide sequence of the gene from *Escherichia coli* K12 and correlations with crystal structures. *J. Biol. Chem.* **263**: 1555–1562.
  7. Chang, W.-S. and J.-S. So. 1999. Characterization of superoxide dismutase in *Lactococcus lactis*. *J. Microbiol. Biotechnol.* **9**: 732–736.
  8. Dukan, S. and T. Nyström. 1999. Oxidative stress defense and deterioration of growth-arrested *Escherichia coli* cells. *J. Biol. Chem.* **274**: 26027–26032.
  9. Gandecha, A. R., S. L. Large, and E. Cundliffe. 1997. Analysis of four tylosin biosynthetic genes from the *tylLM* region of the *Streptomyces fradiae* genome. *Gene* **184**: 197–203.
  10. Geissmann, T. A., M. Teuber, and L. Meile. 1999. Transcriptional analysis of the rubrerythrin and superoxide dismutase genes of *Clostridium perfringens*. *J. Bacteriol.* **181**: 7136–7139.
  11. Hassan, H. M. and I. Fridovich. 1978. Regulation of the synthesis of catalase and peroxidase in *Escherichia coli*. *J. Biol. Chem.* **253**: 6445–6450.
  12. Hopwood, D. A., M. J. Bibb, K. F. Chater, T. Kieser, C. J. Bruton, H. M. Kieser, D. J. Lydiate, C. P. Smith, and J. M. Ward. 1985. *Genetic Manipulation of Streptomyces: A Laboratory Manual*. Norwich: The John Innes Foundation, Colney Lane, Norwich, U.K.
  13. Horinouchi, S., H. Suzuki, and T. Beppu. 1986. Nucleotide sequence of *afsB*, a pleiotropic gene involved in secondary metabolism in *Streptomyces coelicolor* A3(2) and “*Streptomyces lividans*”. *J. Bacteriol.* **168**: 257–269.
  14. Imlay, K. R. C. and J. A. Imlay. 1996. Cloning and analysis of *sodC*, encoding the copper-zinc superoxide dismutase of *Escherichia coli*. *J. Bacteriol.* **178**: 2564–2571.
  15. Ingram, C., M. Brawner, P. Youngman, and J. Westpheling. 1989. *xylE* functions as an efficient reporter gene in *Streptomyces* spp.: Use for the study of *galP1*, a catabolite-controlled promoter. *J. Bacteriol.* **171**: 6617–6624.
  16. Kim, E., H. Kim, S.-P. Hong, K. H. Kang, Y. H. Kho, and Y.-H. Park. 1993. Gene organization and primary structure of a ribosomal RNA gene cluster from *Streptomyces griseus* subsp. *griseus*. *Gene* **132**: 21–31.
  17. Kim, E.-J., H.-P. Kim, Y. C. Hah, and J.-H. Roe. 1996. Differential expression of superoxide dismutases containing Ni and Fe/Zn in *Streptomyces coelicolor*. *Eur. J. Biochem.* **241**: 178–185.
  18. Kim, E.-J., H.-J. Chung, B. Suh, Y. C. Hah, and J.-H. Roe. 1998. Transcriptional and post-transcriptional regulation by nickel of *sodN* gene encoding nickel-containing superoxide dismutase from *Streptomyces coelicolor* Müller. *Mol. Microbiol.* **27**: 187–195.
  19. Kim, E.-J., H.-J. Chung, B. Suh, Y. C. Hah, and J.-H. Roe. 1998. Expression and regulation of the *sodF* gene encoding iron- and zinc-containing superoxide dismutase in *Streptomyces coelicolor* Müller. *J. Bacteriol.* **180**: 2014–2020.
  20. Lee, K. J. 1998. Dynamics of morphological and physiological differentiation in the Actinomycetes group and quantitative analysis of the differentiations. *J. Microbiol. Biotechnol.* **8**: 17.
  21. Markwell, M. A., S. M. Haas, L. L. Bieber, and N. E. Tolbert. 1978. A modification of the Lowry procedure to simplify protein determination in membrane and lipoprotein samples. *Anal. Biochem.* **87**: 206–210.
  22. Meier, B., A. P. Sehn, M. E. Schininà, and D. Barra. 1994. *In vivo* incorporation of copper into the iron-exchangeable and manganese-exchangeable superoxide dismutase from *Propionibacterium shermanii*. *Eur. J. Biochem.* **219**: 463–468.
  23. Park, S.-S. and S.-M. Hwang. 1999. Purification and characterization of iron-containing superoxide dismutase from *Lentinus edodes*. *J. Microbiol. Biotechnol.* **9**: 854–860.
  24. Parker, M. W. and C. C. F. Blake. 1988. Iron- and manganese-containing superoxide dismutase can be distinguished by analysis of their primary structures. *FEMS Lett.* **229**: 377–382.
  25. Prentki, P. and H. M. Krisch. 1984. *In vitro* insertional mutagenesis with a selectable DNA fragment. *Gene* **29**: 303–313.
  26. Rius, N. and A. L. Demain. 1997. Lysine  $\epsilon$ -aminotransferase, the initial enzyme of cephalosporin biosynthesis in Actinomycetes. *J. Microbiol. Biotechnol.* **7**: 95–100.
  27. Sambrook, J., E. F. Fritsch, and T. Maniatis. 1989. *Molecular Cloning: A Laboratory Manual*, 2nd ed. Cold Spring Harbor Laboratory Press, Cold Spring Harbor, NY, U.S.A.
  28. Schnell, S. and H. M. Steinman. 1995. Function and stationary-phase induction of periplasmic copper-zinc superoxide dismutase and catalase/peroxidase in *Caulobacter crescentus*. *J. Bacteriol.* **177**: 5924–5929.
  29. Stallings, W. C., K. A. Patridge, R. K. Strong, and M. L. Ludwig. 1985. The structure of manganese superoxide dismutase from *Thermus thermophilus* HB8 at 2.4-resolution. *J. Biol. Chem.* **260**: 16424–16432.
  30. Steinman, H. M. 1985. Bacteriocuprein superoxide dismutases in pseudomonads. *J. Bacteriol.* **162**: 1255–1260.
  31. Steinman, H. M. and B. Ely. 1990. Copper-zinc superoxide dismutase of *Caulobacter crescentus*: Cloning, sequencing, and mapping of the gene and periplasmic location of the enzyme. *J. Bacteriol.* **172**: 2901–2910.
  32. Storz, G., L. A. Tarataglia, S. B. Farr, and B. N. Ames. 1990. Bacterial defenses against oxidative stress. *Trends Genet.* **6**: 363–368.
  33. Takeda, Y. and H. Avila. 1986. Structure and gene expression of the *E. coli* Mn-superoxide dismutase gene. *Nucleic Acids Res.* **14**: 4577–4589.
  34. Vara, J., M. Lewandowska-Skarbek, Y.-G. Wang, S. Donadio, and C. R. Hutchinson. 1989. Cloning of genes governing the deoxysugar portion of the erythromycin biosynthesis pathway in *Saccharopolyspora erythraea* (*Streptomyces erythreus*). *J. Bacteriol.* **171**: 5872–5881.
  35. Youn, H.-D., H. Youn, J.-W. Lee, Y.-I. Yim, J. K. Lee, Y. C. Hah, and S.-O. Kang. 1996. Unique isozymes of superoxide dismutase in *Streptomyces griseus*. *Arch. Biochem. Biophys.* **334**: 341–348.
  36. Zhang, Y., R. Lathigra, T. Garbe, D. Catty, and D. Young. 1991. Genetic analysis of superoxide dismutase, the 23 kilodalton antigen of *Mycobacterium tuberculosis*. *Mol. Microbiol.* **5**: 381–391.